Journal of Science and Sustainable Development (JSSD), 2026, 14 (1), 60-81

ISSN: 2304-2702 (print); 2414-4479 (online)
DOI: 10.20372/au.jssd.14.2.2026.0753

RESEARCH PAPER

Chickpea Fusarium Wilt (*Fusarium oxysporum* f. sp. *ciceri*): Distribution and Pathogen Characterization in the West and Southwest Shewa Zones in the Oromia Regional State, Ethiopia.

Tsegaye Dabessa[1*], Alemu Lencho[1], Thangavel Selvaraj[1], Jemal Tola[2], and Gezahegne Getaneh[3]
[1]Department of plant Sciences, Ambo University, Ethiopia
[2]Ambo Agricultural Research Center, Ethiopian Institute of Agricultural Research (EIAR);
[3]Debre Zeit Agricultural Research Center, Ethiopian Institute of Agricultural Research
[*]Corresponding Author Email: tsegayedabessa05@gmail.com; ORCID: 0009-0007-2293-7039

Abstract

Fusarium oxysporum f. sp. ciceri, a soil-borne hemi-biotrophic hyphomycete that produces vascular Fusarium wilt,, represents a principal biotic danger affecting the productivity and economic sustainability of chickpea (Cicer arietinum L) production system in Ethiopia. This study studied the contemporary spatiotemporal distribution, field prevalence, environmental causes, and pathogen features of the disease among key smallholder agriculture tracts spanning the West and Southwest Shewa Zones of the Oromia Regional State. Field diagnostic survey data collected from 216 district smallholder plots over two consecutive production cycles (2023/24 and 2024/25) were analyzed using multi-stage cluster descriptive modeling, overlaying disease parameters against localized biophysical parameters, cropping timelines, and host cultivar choices. Survey results confirmed widespread distribution of vascular wilt, with mean disease incidence levels fluctuating markedly between 10.01% and 34.75% across the six investigated districts, demonstrating that intensive monocropping and delayed sowing act as key drivers accelerating regional wilt epidemics. Symptomatic root and stem vascular stands obtained during field samplings identified 70 pure monoconidial fungus cultures on Potato Dextrose Agar (PDA). Quantitative in-vitro radial colony development velocities and microscopic reproductive dimensions were examined via one-way Analysis of Variance (ANOVA) utilizing SAS software's General Linear Models (GLM) method (Version 9.4). The findings indicated that highly significant differences ($p < 0.001$) in radial colony growth velocities on PDA (Grand Mean = 58.42 mm) and colony topography and pigmentation. Diagnostic taxonomic features, such as a large number of oval aseptate microconidia on short monophylies and gently curved macroconidia with 3 to 5 septations, were confirmed by microscopic analyzes. One-way ANOVA for conidial length ($df = 19$, $F = 6940.63$, $p \leq 0.001$) and conidial width ($df = 19$, $F = 647.78$, $p < 0.001$) confirmed deep morphological variability, with mean establishing at 15.82 µm and 5.76 µm respectively. Using the highly susceptible tester line "JG-62" in a Completely Randomized Design (CRD) with three replications, in-vivo pathogenicity testing effectively satisfied Koch's postulates. With grand averages increasing from 8.29% at 30 DAI to 25.61% at 45 DAI and finishing at 44.40% at 60 DAI, two-way ANOVA revealed extremely significant differences ($p < 0.001$) in virulence development. Factorial analysis classified the local isolates into distinct pathogenic groups based on terminal values: 20 highly aggressive (> 70% incidence; maxing out at 93.35%), 40 moderately aggressive (20% - 70% incidence), and 10 weakly aggressive (< 20% incidence) isolates. This study significantly contributes to existing knowledge by shifting from broad, pooled regional pulse disease descriptions to providing the first high-resolution, spatiotemporally mapped micro-level epidemiological blueprint of pathodynamic in Central Ethiopia: Fusarium oxysporum f. sp. ciceri, isolating hyper-virulent local reference standards for targeted, site-specific marker-assisted resistance breeding and sustainable integrated disease management (IDM) frameworks.

Keywords: *Cicer arietinum*, disease survey, host resistance, Koch's postulates, vascular wilt

Introduction

The second most produced pulse crop is the chickpea (*Cicer arietinum* L.) globally, trailing only dry beans, with an international output reaching 17 million tons over a global footprint that has expanded to approximately 14.56 million hectares (FAOSTAT, 2025). Globally, India remains the dominant producer of chickpea, contributing over 73% of the total global production volume (FAOSTAT, 2024). As a dense nutritional repository, chickpea seeds provide an essential, affordable source of plant-based proteins (ranging from 15% to 39% or wider based on cultivar variability), complex carbohydrates, dietary fibers, vitamins, and bioavailable minerals like iron and zinc (Getahun *et al.,* 2021). This comprehensive biochemical profile serves as a critical dietary asset in developing nations combating protein-energy malnutrition (Merga and Haji, 2022). Within the African continent, Ethiopia represents the primary powerhouse for chickpea (*Cicer arietinum* L.) cultivation, processing, and export, commanding approximately 46% of total continental volumetric output (ICARDA, 2019). Nationally, chickpea accounts for more than 12% of the total acreage designated for pulse crops and holds a 14% share of aggregate national pulse production volumes (CSA, 2021), stands as one of the country's most vital food security components (Getahun *et al.,* 2021). Vascular Fusarium wilt caused by the soil-borne, hemi-biotrophic F. oxysporum f. sp. *ciceri* stands out as the yield-limiting threat countrywide, and it is the main cause of this severe productivity gap (Yilma et al., 2026). The epidemiological consequences of this disease are profound; wide-spread localized field surveys reveal baseline disease incidence rates commonly fluctuating between 5% and 58% across major production regions (Yilma eta al., 2026). Depending on the crop phenological stage at initial infection, environmental variables, and cultivar susceptibility, total localized yield losses frequently reach up to100%, often driving smallholders into complete crop failure (Teklu *et al.,* 2024; Yilma *et al.,* 2026).

Resent empirical survey indicate that vascular Fusarium wilt is expanding aggressively in both geographic range and epidemic severity across Ethiopian chickpea-growing jurisdictions (Yimer *et al.,* 2025). Comparative epidemiological investigations conducted across the high-production highland tracs of the Gonder and Gojjam zones documented a parallel, climate-driven intensification of soil-borne fungal complexes, demonstrating that shifts in terminal soil moisture deficits are altering regional Patho system baselines (Yilma *et al.,* 2026). Furthermore, broad-scale surveillance across East African legume ecologies confirms that this aggressive spatial expansion is not isolated to Central Ethiopia; rather, it represents a wider Sub-Saharan phenomenon where rising ambient temperatures during host reproductive phases systematically accelerate xylem colonization rates and shorten the pathogen's incubation window (Assfaw and Negash, 2020). When contrasted with these adjacent regional datasets, the high field intensities documented within the heavy Vertisols of the West and Southwest Shewa Zones underscore an urgent requirement for localized, high-resolution diagnostic mapping. In the West and Southwest Shewa Zones of Oromia, Ethiopia, some attempts were made to understand current status, distribution, and characterization of the chickpea Fusarium wilt pathogen along with the biophysical factors that influence it. In addition, quantitative information on the current status of chickpea Fusarium wilt pathogen disease is lacking and also, due to variability amongst the pathogens, updated information regarding the Fusarium wilt pathogen of chickpeas could be needed. Given the high evolutionary variability, shifting aggressive pathotypes, and persistent nature of this soil-borne hyphomycete, updated regional monitoring is vital for targeted resistance breeding and sustainable integrated disease management (IDM) frameworks. To address these critical epidemiological knowledge gaps, these field, laboratory, and *in-vivo* investigations were initiated to achieve three specific objectives: (i) Determine the contemporary prevalence, field incidence, and internal vascular tissue severity of chickpea Fusarium wilt across the primary production districts of the West and Southwest Shewa

Zones. (ii) Isolate, purify, and morphologically characterize local *F. oxysporum* f. sp. *ciceri* isolates while systematically validating their individual virulence profiles via standard in-vivo pathogenicity testing. (iii) Assess associations between diseases intensity and selected agronomic and environmental factors.

Methods and Materials

Study areas' description

The survey chickpea fields were located in the primary administrative zones of West and Southwest Shewa in the Oromia Regional State, Ethiopia, and ranged in elevation from 2,060 to 2,303 meters above sea level. Six districts from the Southwest and West Shewa administrative zones for this field survey during the October-to-February windows of the 2023/24 and 2024/25 cropping seasons, aligning with the chickpea cultivation cycle in Ethiopia. Three districts were selected from the West Shewa Zone (Dendi, Ejere, and Ejersa Lafo) and three from the Southwest Shewa zone (Sebeta Hawas, Becho, Ilu).

The Agro-ecological and spatial profiles of the surveyed districts were characterized systematically across their respective geographic bounds. In the West Shewa Zone, the study area of Dendi district is bounded by latitudes 09°00.938′ N to 09°02.278′ N and longitudes 38°04.937′ E to 38°12.011′ E, spanning an altitudinal range of 2,199-2,303 m a.s.l., around 85 km to the west of Addis Ababa. The monitored fields in the Ejere district, which is about 46 km west of Addis Ababa, covered elevations between 2,081 and 2,180 m a.s.l. and were bounded by latitudes 08°58.244′ N to 09°01.555′ N and longitudes 38°19.738′ E to 38°20.996′ E within the same zone. Sown chickpea stands were found at an altitudinal range of 2,110 to 2,170 m a.s.l. in the nearby Ejersa Lafo district, which is roughly 60 km west of Addis Ababa. Their coordinates fell between latitudes 08°59.154′ N and 09°00.443′ N and longitudes 38°13.820′ E and 38°17.758′ E. At the same time, different Agro-climatic clusters were identified using spatial monitoring throughout the Southwest Shewa Zone. Sown stands in the Becho district, situated approximately 82 km Southwest of Addis Ababa, featured an altitudinal profile ranging from 2,112 to 2,156 m a.s.l., and were bounded by altitudes 08°40.233′ N to 08°43.105′ N and longitudes 38°13.587′ E to 38°16.112′ E. Moving closer to the capital, the field assessment points in the Ilu district fell within narrow altitudinal bands of 2,060 to 2,091 m a.s.l., bounded by latitudes 08°46.731′ N to 08°49.332′ N and longitudes 38°19.220′ E to 38°22.545′ E, situated roughly 55 km Southwest of Addis Ababa. Finally, the Sebeta Hawas district, positioned approximatel y 26 km southwest of Addis Ababa, contained monitored production fields at altitudinal elevations between 2064 and 2083 m a.s.l., traversing a spatial grid bounded by latitudes 08°49.162′ N to 08°50.205′ N and longitudes 038°30.457′ E to 038°31.854′ E (Fig. 1).

Survey design and sampling strategy

The multi-stage purposive sampling framework was executed systematically across the selected districts by targeting three major kebeles (farmer associations) per administrative unit based on intensive chickpea production histories. Field monitoring was carried out in the kebeles of Yubido Legebatu, Dano Ejersa Gibe, and Awash Bolo within the Dendi district; Kimoye, Enaftu, and Tulu Korma within the Ejere district; and Jemijem Legebatu, Cheleleka Bobe, and Serewa Debisa in the neighborhood of Ejersa Lafo.

At the same time, agricultural monitoring in the nearby Southwest Shewa Zone monitored production fields in the districts of Becho (Batu, Kobo, and Awash Bune); Ilu (Bili, Keta Asgori, and Buti Talgo); and Sebeta Hawas (Borohiro, Debelyohans, and Nanotefki). This spatial distribution guaranteed an even geographical spread across both administrative zones, capturing localized smallholder farming micro-climates and management variations cleanly. Within each designed kebeles, twelve smallholder production fields were evaluated.

Field monitoring operations were stratified equally across two consecutive cultivation cycles, tracking 108 production fields in the 2023/24 season and an additional 108 fields in the 2024/25 season. This framework generated a cumulative national sample matrix of 216 unique production environments for statistical evaluation. The structural allocation of the cumulative sample size (N = 216) was mathematically derived via a multi-stage cluster configuration according to the following sampling hierarchy:

2Administrative zones × 3districts per zone × 3kebeles per district × 6fields per kebele per year × 2cropping cycles = 216 fields.

The multi-year sample footprint of 216 unique production environments was considered highly adequate to rigorously represent the targeted epidemiological landscape based on three interconnected spatial-statistical parameters. First, the purposive selection of these specific fields across an altitudinal gradient of 2,060 to 2,303 m a.s.l. ensured the saturation of biophysical variation, effectively capturing the full range of microclimatic regimes, soil-moisture variations, and thermal zones that govern *Fusarium oxysporum* f. sp. *ciceri* pathodynamic in Central Ethiopia. Second, this sampling scale strictly fulfills established epidemiological replication guidelines; according to foundational plant disease epidemiology survey principles (Campbell and Madden, 1990; Yimer *et al.*, 2025), a multi-seasonal matrix exceeding 150 to 200 field observation points generates sufficient degrees of freedom (df) within the statistical Analysis of Variance (ANOVA) error matrix to cleanly isolate genuine pathotypic, agronomic, and geographic effects from confounding environmental noise. Finally, by tracking precisely 12 smallholder fields per kebele over two consecutive years, the framework achieved a thorough representation of localized farming practices, successfully integrating the diverse sowing chronologies, micro-plot organic amendment application rates, and historical cereal-legume crop rotation sequences (predominantly involving teff and wheat) that directly dictate soil-borne chlamydospore inoculum densities and suppressive rhizosphere dynamics within these high-intensity chickpea production belts.

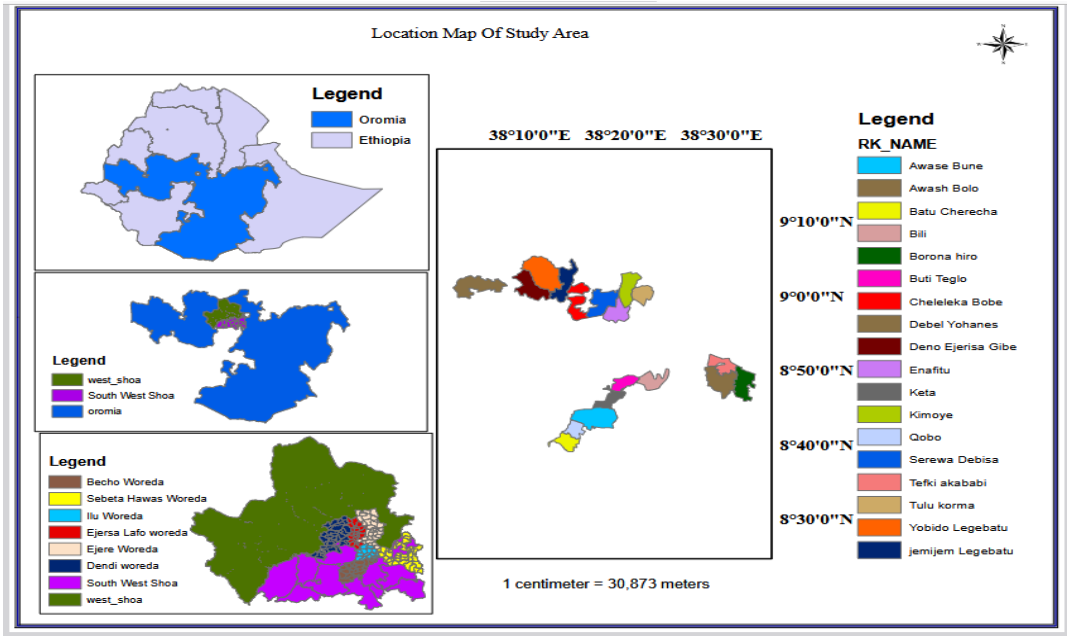

Figure 1. Geographic location map of the study districts and sampled smallholder chickpea fields across the West and Southwest Shewa Zones of the Oromia Regional State, Ethiopia.

Map borders are delineated in standard geographic coordinates using North (N) and East (E) directional suffixes (RK: Rural Kebeles, indicating the lowest local administrative tier in the rural districts of Ethiopia).

Survey procedures and biophysical factors tracking

Monitored smallholder fields within each target district were intercepted along primary and secondary feeder agricultural transit roads at predetermined linear intervals of at least 5 km in order to guaranty a representative and non-overlapping spatial distribution. To fully monitor seasonal epidemics, field surveys started in the early host vegetative phase and continued through the complete crop pod-setting growth phases. A portable Geographical Position System (GPS) receiver was used at each diagnostic sampling site to record exact altitudinal measurements and geographic coordinates. In order to monitor local biophysical factors, a structured agronomic ledger was created concurrently.

Based on morphological characteristics, the host crop type was classified as either conventional Desi or improved, large-seeded Kabuli kinds. Furthermore, in order to clearly distinguish between continuous monocropping and varied cereal-legume rotations, local cropping histories were recorded to capture the immediately previous crop rotation cycles. Visual and textural classification were also used to assess soil matrix profiles, and it was found that heavy clay Vertisols predominated in the areas under observation. Lastly, crop phenological growth stages were methodically assessed, and the exact host growth phase during each observation window was ascertained using conventional decimal keys (Fig. 2).

Figure 2. Photos taken at the research locations in 2023 and 2024 G.C. during the field survey, sample collection (A), and GPS data recording (B).

Qualitative disease sampling was accomplished by systematically touring each producing fields using an inverted diagonal "W" transect pattern to reduce edge effects and minimize spatial bias. At five randomized equidistant places along the transect, a 1 m^2 quadrat was deployed to quantify disease parameters. Individual quadrat metrics were subsequently pooled and synthesized to derive a single, mathematically robust mean value for each operational farm matrix. Symptomatic root and lower stem specimens exhibiting definitive diagnostic indicators of vascular wilting such as severe chlorosis, downward epinasty, and internal xylem browning were carefully excavated along with healthily control plants from each site.

Collected tissue specimens were immediately transferred into clean, breathable paper envelopes, placed inside labeled polyethylene storage bags, and maintained within insulated coolers at 4ºC to arrest secondary decay. All specimens were transported to the Plant Pathology Laboratory at Ambo University.

Disease assessment

The spatiotemporal distribution, prevalence, and field intensities of the wilt epidemics were quantified across all 216 monitored farms using three standardized epidemiological parameters:

Disease prevalence

The disease prevalence was calculated by dividing the number of quadrats showing the disease by the total number of quadrats evaluated in each field, and this value was subsequently converted to a percentage. The subsequent description details the method used to calculate the disease prevalence. The ratio of the number of quadrats impacted by the disease to the total number of quadrats evaluated in each field, multiplied by 100.

Prevalence of disease (%) = The count of quadrats impacted by the disease / The total count of quadrats evaluated in each field × 100.

Incidence of disease

The incidence of chickpea Fusarium wilt was calculated by dividing the number of infected plants in a chosen quadrat by the total number of plants assessed within that quadrat and expressing the result as a percentage. The average incidence of disease across the five quadrats in each field was calculated. The incidence of disease (%) is calculated as follows: The total of withered chickpea plants within a quadrat / the total of plants evaluated within that quadrat × 100.

To assess the severity of the disease, five chickpea plants were randomly uprooted from each quadrat and examined for internal vascular discoloration. The percentage of root vascular bundle necrosis was scored using a modified 0-4 descriptive scale, where Grade 0 represented 0% vascular infection (completely symptomless), Grade 1 indicated 1-25% vascular infection or slightly discoloration, Grade 2 signified 26-50% vascular infection or moderate discoloration, Grade 3 denoted 51-75% vascular infection or extensive discoloration, and Grade 4 represented 76-100% vascular necrosis, characterized by complete tissue death or absolute structural wilt. The individual plant scores were subsequently averaged per quadrat and aggregated to establish a structurally sound estimate of disease severity per field. This rigorous scoring framework builds upon foundational visual indices modified for recent pulse crop pathodynamic (Teklu *et al*., 2024).

Meteorological data acquisition

To model regional macro-climatic influences on wilt progression, localized monthly weather records covering the 2023 and 2024 growing seasons were obtained from the National Meteorology Agency of Ethiopia. The gathered datasets included cumulative monthly precipitation, mean relative humidity, and monthly maximum/minimum ambient temperatures. Environmental profiling targeted the window from August to December to capture pre-planting soil moisture retention through to critical host phenological development phases (Table 1).

Table 1. Meteorological profiles recorded from surveyed zones during 2023/24 and 2024/25 cropping seasons.

Year	Parameter	Aug.	Sept.	Oct.	Nov.	Dec.	Jan.	Feb.	Mean
2023/24	Mean RF (mm)	257.10	140.52	89.95	36.76	12.88	6.46	20.17	85.60
	Mean RH (%)	73.56	72.63	66.03	63.28	57.44	57.40	59.29	64.20
	Max. Temp. (°C)	28.30	28.40	28.40	29.40	29.30	29.90	31.30	29.20
	Min. Temp. (°C)	2.10	3.20	2.20	2.10	0.10	2.40	4.10	2.30
2024/25	Mean RF (mm)	200.34	119.06	67.64	30.67	13.87	1.96	4.18	62.50
	Mean RH (%)	67.90	67.89	59.35	59.67	55.05	51.75	49.35	58.70
	Max. Temp.(°C)	31.00	29.50	30.70	30.00	29.70	31.00	32.00	31.50
	Min. Temp. (°C)	2.90	5.80	5.30	3.30	1.00	-0.20	5.20	3.30

Source: - From Ethiopia National Metrology Agency.

Isolation and characterization of the fungal pathogen

To isolate the causal phytopathogens, systematic chickpea plants exhibiting pathognomonic vascular wilt indicators were collected from 108 production fields across the West and Southwest Shewa Zones of the Oromia Regional State, Ethiopia. The root system were meticulously washed under distilled water to dislodge adhering rhizosphere soil and structural debris, followed by blot-drying between sterile filter paper layers. Tissue fragments measuring approximately 2-3 mm were excised from the advancing margins of internal vascular discoloration using a sterile scalpel blade. To eliminate superficial saprophytic microorganisms, the root segments were surface sterilized for one minute in a 2% sodium hypochlorite (NaOCl) solution. Any leftover chemical residue was then rinsed three times in sterile distilled water before being blotted dry. Five tissue segments were equally spaced throughout standard Potato Dextrose Agar (PDA) matrices. The plates were incubated at 28 ± 2°C for seven days in order to encourage early hyphal growth (Aneja, 2003). Single-spore isolation and hyphal-tip extraction methods were used to create axenic fungal cultures. Active mycelial disks from the advancing colony boundaries were transferred onto new PDA plates using a flamed inoculating loop to do sub-culturing under aseptic conditions. This purification process was carried out repeatedly until clean, morphologically homogeneous parental colonies were produced. For further research, pure cultures were kept at 4 °C on PDA slants in sterile screw-capped test tubes (Kurt *et al.,* 2002). In accordance with the standard foundational guidelines for Fusarium species, the pure *Fusarium oxysporum* f. sp. *ciceri* isolates were taxonomically confirmed using diagnostic culture and macro-morphological criteria, such as radial mycelial growth velocities, colony margin architecture, surface coloration, and reverse pigmentation matrices (Leslie and Summerell, 2006).

Fungal spores were aseptically put on glass slides for microscopic characterization, dyed with lactophenol cotton blue (or methyl blue), covered with a coverslip, and examined using a stereo binocular microscope at 40× and 100× magnifications at the Ambo Agricultural Research Centre. Diagnostic parameters captured included macro-conidial geometric curvature, micro-conidial arrangements on short monophylies, and the presence, position, or wall texture of chlamydospores. The recorded morphological profiles were cross-referenced against established mycological diagnostic keys and standard taxonomic criteria to confirm definitive placement within the *Fusarium oxysporum* species complex (Leslie and Summerell, 2006).

Inoculum mass multiplication and pathogenicity verification

Mass multiplication of *Fusarium oxysporum* f. sp. *ciceri* on sorghum grains

Axenic cultures of the purified *Fusarium oxysporum* f. sp. *ciceri* isolates were mass-

multiplied on whole sorghum (*Sorghum bicolor* L.) grains as a solid substrate. The sorghum grains were soaked overnight in distilled water, drained of excess moisture, and transferred into (500 mL) conical flasks. The flasks were sealed with non-absorbent cotton plugs and sequentially autoclaved at 121°C (15 psi) for 30 min over two consecutive days. Upon cooling to room temperature, each flask was aseptically inoculated with a 5mm mycelial disc excised from the advancing margins of actively growing 5-day-old Potato Dextrose Agar (PDA) cultures. The inoculated flasks were incubated at 25 ± 2°C for 15 days in the Plant Pathology Laboratory at Ambo University. To ensure uniform fungal colonization, prevent particle clumping, and accelerate substrate penetration, the flasks were manually agitated daily throughout the incubation window. Fully colonized grain substrates were deployed for downstream pathodynamic validation (Fig. 3).

Figure 3. Mass Multiplications of *Fusarium oxysporum* f. sp. *ciceri* inoculum on Sorghum grains that were used for pathogenicity test at Ambo University, plant pathology laboratory.

Pathogenicity testing and Koch's postulates verification

Greenhouse pathogenicity tests were conducted to systematically verify fulfillment of Koch's postulates using the highly susceptible tester variety 'JG-62'. Steam-sterilized soil matrix (2 kg) was put into plastic pots with a diameter of 25 cm. The solid-state sorghum inoculum was thoroughly incorporated into the soil profile at a standardized amendment rate of (200 g kg^{-1}) of soil achieving a target population density of approximately (10^8cfug^{-1}). The infested soil mixtures were lightly moistened and incubated for 4 days prior to planting to facilitate initial fungal stabilization. In three separate biological replications, five surface-sterilized "JG-62" seeds were planted per pot. To maintain a uniform moisture profile ideal for symptoms of disease while preventing saturated conditions, the pots were watered once a week. Symptomatic progress characterized by leaf chlorosis, downward epinasty, and progressive wilting was quantitatively monitored at 30, 45, and 60 days post-sowing. Causal pathogen identity was systematically confirmed by re-isolating the fungal agent from the vascular tissues of symptomatic host roots exhibiting characteristic internal xylem discoloration, which verified compliance with Koch's postulates by matching the cultural and macro-morphological traits of the parental axenic stock (Jamil and Ashraf, 2020).

Pathogenicity screening and inoculation protocol

The pathogenic variability of 70 isolates of F. oxysporum f. sp. ciceri and one uninoculated sterile soil with three replications in two cycles (September-December 2024 and 2525), totaling 213 pots, was investigated at room temperature in a controlled greenhouse at Ambo University using plastic pots (30 cm in diameter) arranged in a Completely Randomized Design (CRD). Healthy seeds originating from the extremely vulnerable chickpea cultivar "JG-62" were surface sterilized for three minutes using 1% sodium hypochlorite (NaOCl), thoroughly rinsed 3 times with sterile distilled water, and air dried. The fungus was grow on a sand-maize meal medium (9:1 w/w ratio) for 14 days at 25±2°C until a large number of chlamydospores and conidia were formed in order to prepare the inoculum for each isolated strain. The substrate was added to an autoclaved soil mix (soil: sand: peat moss at 2:1:1 v/v/v) at a consistent rate of 10% (w/w). The control block consisted of non-inoculated pots that contained only the autoclaved soil mix. The 25 cm diameter plastic pots have been filled with two kg of steam-sterilized soil. To ensure equitable distribution, the mass-multiplied fungus was added to these pots at a rate of 200 g kg^{-1} (10^8 $cfug^{-1}$) soil and thoroughly mixed. The pots were incubated for four days and, if needed, occasionally watered. Each pot sown 5 surface-sterilized seeds of the chickpea cultivar "JG-62," for a total of 15 plants per treatment in each of the three replicates (Fig. 4). The minimal moisture requirements of the plants were satisfied by watering the containers once a week.

Figure 4. Pathogenicity test activity in chickpea cultivar 'JG-62' at Ambo University, greenhouse conditions.

Spatiotemporal disease monitoring and incidence computation

At 30, 45, and 60 Days After Inoculation (DAI), the progressive spatiotemporal expansion of Fusarium wilt symptoms which were initially characterized by lower leaf yellowing, flaccidity, marginal necrosis, petiole drooping, and ultimately Fusarium vascular wilting was methodically observed and recorded. The disease incidence percentage (PDI) within each replicate pot was calculated as the proportion of plants displaying visible localized or systemic wilt symptoms in relation to the total number of plants that emerged. The following conventional epidemiological formula was used to compute the spatiotemporal progress of chickpea Fusarium wilt incidence (%) for each replication matrix (Jamil and Ashraf, 2020).

$$\text{PDI} = \frac{\text{Number of wilted plants per pot}}{\text{Total number of plants per pot}} \times 100$$

Statistical analysis

In order to describe the spatiotemporal distribution and relative importance of chickpea wilt diseases across the districts, survey data were summarized and analyzed using descriptive statistics. Based on the approximate similarity of the variables to the total assessed fields in each zone, class boundaries were chosen for disease incidence and severity data separately. To analyze the relationship between wilt disease pathogen and biophysical factors, disease incidence and severity were classified into district class boundaries (Yuen, 2006). The effect of the independent variables on the disease's incidence and severity has been evaluated twice. The relationship between the incidence, severity, temperatures, relative humidity, and rainfall during the survey period in 2023 and 2024 was investigated in order to classify and rank districts into wilt risk areas. SAS version 9.4 (SAS Institute Inc., 2017) was used for the statistical analyzes in this study. Either the Analysis of Variance (ANOVA) or General Linear Models (GLM) methods were used to examine the data. Duncan's Multiple Range test and Fisher's Protected Least Significant Difference (LSD) test with $P \leq 0.05$ were utilized for comparing means. To assess variations in disease intensity among districts, cropping seasons, and host varieties, descriptive statistics were used to summarize spatiotemporal survey data and biophysical factors, which were then submitted to Analysis of Variance (ANOVA). Pearson correlation coefficients r was computed to quantify relationships between environmental drivers (meteorological profiles, elevation, crop rotation sequences) and disease metrics (Teklu *et al.,* 2024). Using the Linear Model recommendations for a Completely Randomized Design, a conventional Analysis of Variance (ANOVA) was performed on all accumulated spatiotemporal replication percentages. Localized replicate fluctuations (e.g., scoring variations of 40% and 46.66% inside certain blocks) were kept to compute the correct Mean Square Error (MSE) in order to satisfy mathematical compliance for hypothesis testing and correct structural zero-variance bounds. The Least Significant Difference (LSD) test at a 95% Confidence Level ($\alpha = 0.05$) was used to distinguish treatment. The experimental reliability and degree of precision were determined by computing the Coefficient of Variation (CV %) for each chronological window:

$$\text{CV}\ (\%) = \sqrt{\frac{\text{Mean Square Error}}{\text{Grand Mean}}} \times 100$$

All generated pathodynamic percentage datasets were subjected to standard checking procedures to verify normal distribution variance assumptions. Factorial Analysis of Variance (ANOVA) procedures utilizing SAS software (version 9.4) were used to process the data. Terminal disease incidence means recorded at the final 60 DAI evaluation boundary were utilized to cluster the isolates into four distinct pathotype categories: Highly Pathogenic (>70%) final wilt incidence), Moderately Pathogenic (20% - 70%), Slightly Pathogenic (<20%), and non-pathogenic (0%).

Results

Spatiotemporal distribution and intensity of Fusarium wilt

Systematic diagnostic field surveys demonstrated that vascular wilt symptoms were distributed throughout the major chickpea-producing belts of Central Ethiopia. The target pathogen was detected in 152 out of the 216 fields assessed across the 2023 and 2024 cropping seasons, establishing an overall regional prevalence of 70.36%, a mean disease incidence of 23.96%, and an average severity rate of 21.43%. ANOVA showed statistically significant differences ($p < 0.05$) in disease parameters across the six surveyed districts (Table 2 and Fig. 5).

Among the monitored smallholder networks, Becho district within the Southwest Shewa zone exhibited the highest mean disease incidence at 34.75% ± 1.25%. This was followed closely by Dendi district in the West Shewa zone, which recorded a mean incidence of 31.20% ± 1.18%. Statistically, the wilt incidence values for Becho and Dendi belonged to the same superior

significance group. Converse At 10.01% ± 0.72%, the Ejersa Lafo district had the lowest field disease incidence. Regarding internal tissue damage, peak disease severity was recorded within Becho district at 27.43% ± 1.15%, which statistically surpassed the structural severity noted in Dendi at 25.10% ± 1.10%.The absolute minimum disease severity was tracked in Ejersa Lafo at 10% ± 0.65%.

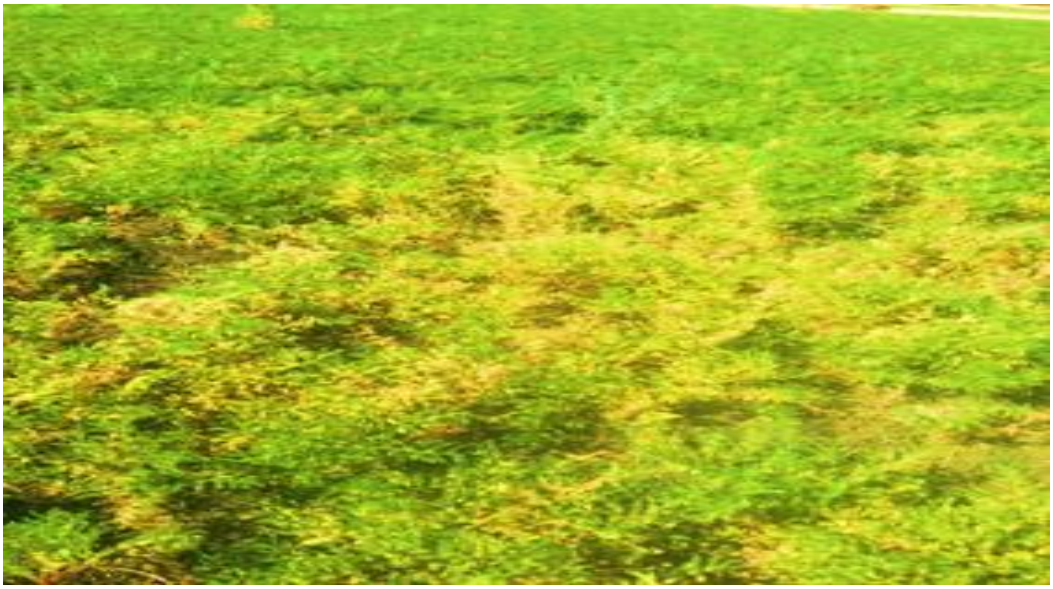

Figure 5. Farmer's chickpea field infection of *F. oxysporum* f. sp. *ciceri* showing typical wilting, at Becho district, Ethiopia, during field investigation

Table 2. Mean Fusarium wilt prevalence, incidence, and severity in chickpeas across six districts and altitude ranges in West and Southwest Shewa, Ethiopia during the 2023 and 2024 cropping seasons.

Districts	Altitude (m.a.s.l.)	Fields Assessed	Fields Affected	Prevalence (%)	Disease Incidence (%)*	Disease Severity (%)*
Dendi	2,199-2,303	36	30	83.33^{a}	31.20 ± 1.18^{a}	25.10 ± 1.10^{a}
Ejere	2,081-2,180	36	25	69.44^{ab}	23.91 ± 1.05^{b}	20.37 ± 0.92^{b}
Ejersa Lafo	2,110-2,170	36	16	44.44^{b}	10.01 ± 0.72^{d}	10.00 ± 0.65^{d}
Becho	2,112-2,156	36	31	86.11^{a}	34.75 ± 1.25^{a}	27.43 ± 1.15^{a}
Ilu	2,060-2,091	36	28	77.78^{a}	25.40 ± 1.12^{b}	22.80 ± 0.95^{ab}
Sebeta Awas	2,064-2,083	36	22	61.11^{ab}	18.50 ± 0.98^{c}	16.45 ± 0.88^{c}
Total Mean		216	152	70.36	23.96	21.43
SD				26.37	8.96	7.43
SE of Mean				10.74	3.66	3.03

Note: Duncan's Multiple Range test indicates that there is a significant difference ($p < 0.05$) between means in the same column that are followed by different superscript letters. m.a.s.l. = meters above sea level.

Cultivar susceptibility variations

A clear variation in disease expression was observed between different crop types across both seasons. Local Desi-type cultivars exhibited a mean disease incidence of 29.85% and a severity score of 26.40%. In contrast, fields planted with improved Kabuli-type cultivars demonstrated mean disease incidence metrics restricted to 15.12% and severity scores restricted to 14.10%.

Influence of host phenology and biophysical factors.

Wilt intensity rose with host development from vegetative initiation to reproductive maturity. Disease markers reached an average incidence of 8.2% at the establishment stage, 18.5% during the vegetative phase, and peaked at 26.0% during the late full-podding and crop ripening phases. Pearson correlation modeling mapped the relationship between environmental or biophysical variables and chickpea Fusarium wilt intensity metrics across the target zones (Table 3).

Table 3 Person correlation coefficient (r) mapping the relationship between environmental/ biophysical variables and chickpea Fusarium wilt intensity metrics.

Biophysical variables	Disease Incidence (r)	Disease Severity (r)	Significance Level (p)
Mean Seasonal Temperature (°C)	0.68	0.65	< 0.01
Elevation / Altitude Range (m)	0.42	0.47	< 0.05
Preceding Crop Sequence (Teff/Barley)	0.53	0.51	< 0.05
Seasonal Total Precipitation (mm)	-0.54	-0.50	< 0.01
Relative Humidity (%)	-0.48	-0.42	< 0.01

There was a significant positive association between mean seasonal temperature and both disease incidence ($r = 0.68$, $p < 0.01$) and structural severity ($r = 0.065$, $p < 0.01$).

This demonstrates that fungal development is significantly accelerated by higher temperature s. Additionally, altitude had a positive correlati on with both severity ($r = 0.47$, $p < 0.05$) and incidence ($r = 0.42$, $p < 0.05$). This suggests that environmental changes related to altitude have an impact on chickpea Fusarium wilt in these producing zones. Additionally, historical cropping sequences that included continuous monocultural of cereal crops like barley or teff showed a high connection with increasing sickness incidence ($r = 0.53$, $p < 0.05$) and severity ($r = 0.51$, $p < 0.05$). Conversely, the incidence ($r = -0.54$, $p < 0.01$) and severity ($r = -0.50$, $P < 0.01$) of symptoms were negatively correlated with cumulative seasonal precipitation. Relative humidity, which functioned as a limiting environmental factor against the progression of symptoms, matched this trend ($r = -0.48$, $p < 0.01$).

Influence of host plant growth stages on disease expression

Amongst the fields investigated, 32.4% were in the vegetative stage, 42.6% were in the flowering stage, 15.74% were in the podding stage, and 9.26% were in the full podding stage. Field observations showed that disease incidence was 18.1% during the vegetative stage, 21.7% during the flowering stage, 23.4% during the podding stage, and peaked at 26.0% at the full podding or ripening stage. This trend demonstrates that as host plant development progresses, the visible intensity of chickpea wilt increases. Rising temperatures and transpiration pull during the reproductive stage accelerate fungal proliferation and vascular clogging within host tissues, leading to acute symptom expression. This is supported by Assfaw and Negash (2020), who demonstrated that the intensity of chickpea vascular wilt in Ethiopia varies significantly under the influenc e of local microclimates, host phenological growth stages, altitudinal gradients, cultivar selections, and historical crop rotation sequence s; these spatiotemporal and biophysical dynami cs have been further corroborated by recent macro-scale survey assessments across regional legume production belts (Yimer *et al.* 2025; Yilma *et al.* 2026).

Variation in disease intensity driven by preceding cropping sequences

The type of crop grown prior to chickpea cultivation significantly influenced Fusarium wilt incidence across the surveyed fields. The average disease incidence in 24 fields with a maize–chickpea cropping system was 20.18%, whereas 50 fields with a wheat–chickpea cropping system showed a mean incidence of 13.25%. Two fields utilizing a common bean–chickpea cropping system showed a low average disease incidence of 2.38%, and two fields with a beetroot–chickpea system exhibited an average incidence of 5.71%. In contrast, two fields with a green pepper–chickpea system showed an average incidence of 21.98%. High disease values were recorded in four fields under a barley–chickpea system (24.73% incidence) and 132 fields under a teff–chickpea system (24.64% incidence). The finding that barley–chickpea and teff–chickpea systems support high wilt levels is consistent with Srinivas (2016), who found that the choice of cropping methods and rotation histories significantly alters soil-borne disease incidence.

Similarly, Rani *et al*. (2017) found that high disease incidence is closely linked to preceding crops that act as alternative hosts or create rhizosphere conditions that aggravate the pathogen. In fields where chickpeas follow specific cereal crops, root exudates can stimulate *F. oxysporum* chlamydospore germination, maintain high soil inoculum levels and increase disease pressure in subsequent seasons. Wilt scores expanded as crops advanced from vegetative (18.1% incidence) to full podding/ripening stages (26.0%). Preceding crop configurations heavily dictated disease pressure (Table 4 & 5). Cereal rotations generated the highest wilt values, led by barley–chickpea (24.73% incidence) and teff–chickpea systems (24.64%), whereas common bean–chickpea rotations restricted incidence to a low of 2.38%. This indicates that certain crop sequences yield root exudates that restrict *F. oxysporum* spore germination.

Table 4. Influence of preceding crop rotation cycles on chickpea Fusarium wilt parameter .

Crop kinds that came before	Field frequency (*n*)	Configuration of the primary agricultural system	Mean disease incidence (%)
Barley	4	Chickpea-Barley system	24.73
Teff	132	Chickpea-Teff system	24.64
Green Pepper	2	Chickpea-Green Pepper system	21.98
Maize	24	Chickpea-Maize system	20.18
Wheat	50	Chickpea-Wheat system	13.25
Beetroot	2	Chickpea-Beetroot system	5.71
Common Bean	2	Chickpea-Common Bean system	2.38
p-value			< 0.0001 (***)

Table 5. shows the average frequency and percentage severity index (PSI) of Fusarium wilt of chickpea for various independent variables throughout the cropping seasons of 2023/24 and 2024/25 .

Variable	Variable class	Inc. Mean ± SD	PSI (Mean ±SD)
District	Dendi	31.20 ± 1.18	25.10 ± 1.10
	Ejere	23.91 ± 1.05	20.37 ± 0.92
	Ejersa Lafo	10.01 ± 0.72	10.00 ± 0.65
	Becho	34.75 ± 1.25	27.43 ± 1.15
	Ilu	25.40 ± 1.12	22.80 ± 0.95
	Sebeta Awas	18.50 ± 0.98	16.45 ± 0.88
p-value		< 0.0001 (***)	< 0.0001 (***)
Planting date	Early	36.69 ± 13.9	24.06 ± 10.95
	Late	42.89 ± 18.28	20.28 ± 10.54

p-value		0.0241 (*)	0.0185 (*)
Crop density	≥30plant/1m^2	14.97 ± 4.48	6.20 ± 2.58
	<30plant/1m^2	14.47± 4.87	5.73 ± 2.74
p-value		0.4682 (NS)	0.3155 (NS)
Growth stage	Vegetative	18.1± 5.04	7.24 ± 3.73
	Flowering	21.7± 9.87	20.23 ± 12.42
	Podding	23.4± 11.97	26.38 ± 10.78
	Fully podding	26± 12.41	30.68 ± 11.33
p-value		0.0014 (**)	< 0.0001 (***)
Previous crop	Teff	24.64± 9.91	25.61 ± 10.95
	Maize	20.18± 9.78	18.28 ± 8.54
	Wheat	13.25± 4.74	6.40 ± 2.71
	Barely	24.6 ± 10.91	26.06 ± 9.55
	Common bean	2.38± 1.45	4.53± 2.90
	Beet-root	5.71± 3.47	5.33± 3.24
	Green paper	21.98± 13.21	25.61 ± 10.65
p-value		< 0.0001 (***)	< 0.0001 (***)

*Significant levels: NS: Non-Significant ($p > 0.05$); ***Highly Significant ($p < 0.0001$); **Significant ($p < 0.01$); * Significant ($p < 0.05$); Inc. stands for incidence, SD for standard deviation, and PSI for percentage severity index.

Characterization of the pathogens

In order to monitor radial growth kinetics and pigment synthesis under a regulated photoperiod arrangement, axenic cultures obtained from symptomatic vascular tissues were transplanted onto selective medium configurations. When *Fusarium oxysporum* f. sp. *ciceri* was cultured on regular Potato Dextrose Agar (PDA), colonies showed symmetrical, fast radial development with sparse to moderately thick aerial mycelia. With a distinctive white-to-creamy color that progressively changed into light pink or pastel violet as the culture developed, the surface texture seemed cottony to floccose. The reverse side of the plates revealed a definiteve dark violet-to-magenta water-soluble pigmentation concentrated beneath the advancing margin. *Fusarium solan:* on PDA, colonies exhibited a distinctly denser, felt-like aerial mycelial mat compared to Foc, with a cream, white, or distinct bluish-grey surface presentation. The reverse side of the plate produced a prominent blue-green, olive, or dark coffee-brown pigmentation matrix, providing an immediate macroscopic filter to distingush it from the pink-violet hues of Foc. Bacterial Wilt (*Ralstonia solanacearum*): Tissue extracts were streaked onto Triphenyl Tetrazolium Chloride (TZC) Agar medium by Kelman.

After incubation at 30°C for 48 hours, R. solanacearum produced highly fluid, irregularly shaped, smooth, mucoid colonies. These colonies displayed a creamy-white coloration with highly diagnostic swirling pink-to-deep-red centers, confirming the presence of virulent, extracellular polysaccharide-producing bacterial cells rather than fungal structures. Based on the above identification criteria out of 108 samples initially cultured in PDA medium during pathogen isolation, all the isolates were purified, and the results obtained from this study showed that 70 isolates were regarded as *Fusarium oxysporum* f. sp. *ciceri*, 15 of them were *F. solani* and 5 of the isolates were bacterial wilt and 18 of the isolates were unidentified because not grown in PDA medium during isolation and out of the total 70 pure isolates were investigated under pathogenicity test assessment only 20 isolates were grouped under highly pathogenic and this 20 isolates were used for morphological examination under microscopic at Ambo Agricultural Research Centre, Ethiopia (Fig. 6).

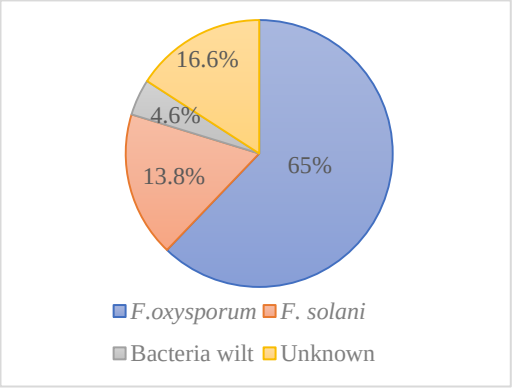

Figure 6. Percent isolation of chickpea wilt causing pathogens identified from root samples collected from West and Southwest Shewa Zones of Oromia, Ethiopia.

Pathogenicity and aggressiveness of fungal isolates

The initial symptoms usually shown within 30 days after chickpea seeds were sown on inoculated soils up as discoloration on the lower leaves and twigs, and the leaves of the plant that was infected were dropped to the ground. Within a few days, entire plants exhibit withering and collapse. Light yellow, leaf drop, and finally host wilting were the primary symptoms to appear. Partial wilt occurs in some of the isolates and certain plants are affected and show symptoms within 30 days of sowing, with affected seedlings exhibiting drooping leaves followed by complete plant death. Even though the roots appeared healthy, a vertical break shows brown to black discoloration in the vascular tissues. When compared originally diseased and wilted chickpea plants in the field, the wilting symptoms caused by the artificially infected and diseased plants were identical and confirmed.

The isolates were categorized into three groups based on wilting percentage in pathogenicity tests. The findings indicated that amongst the 70 samples examined using the *F. oxysporum* f. sp. *ciceri* pathogenicity test, 20 samples produced the greatest disease incidence on 'JG-62'and grouped as highly pathogenic (>70%) final wilt incidence), 40 isolates were showing medium disease incidence and grouped as moderately pathogenic (20%-70%), and 10 isolates were showing low disease incidence and grouped as slightly pathogenic (<20%), and zero non-pathogenic (0%). With ultimate wilt incidence levels ranging from 20% to 70%, the moderately pathogenic group comprised an extended cluster of 40 isolates that showed increasing symptom progression. This group averaged 42.22% final wilt incidence and included 15 calibrated strains (Foc-28, Foc-30, Foc-38, Foc-58, Foc-67, Foc-69, Foc-70, Foc-84, Foc-89, Foc-91, Foc-93, Foc-95, Foc-97, Foc-103, and Foc-107) alongside Foc-1, Foc-2, Foc-3, Foc-6, Foc-8, Foc-10, Foc-12, Foc-14, Foc-15, Foc-16, Foc-18, Foc-21, Foc-22, Foc-31, Foc-34, Foc-47, Foc-48, Foc-78, Foc-79, Foc-79, Foc-80, Foc-81, Foc-85, Foc-87, Foc-102 and Foc-108. On the other hand, ten low-virulence isolates (Foc-24, Foc-62, Foc-64, Foc-65, Foc-66, Foc-72, Foc-75, Foc-92, Foc-96, and Foc-104) were found in the somewhat pathogenic group, which was defined by a final wilt incidence below 20%. Finally, the non-pathogenic group (0% wilt incidence), represented by the non-inoculated control block, remained entirely disease-free throughout the 60-day evaluation matrix, confirming the structural integrity of the bio-assays and the complete absence of cross-contamination across treatments. The chickpea wilt symptoms that were observed were comparable to those that were previously identified from the fields which had been examined. Koch's postulates were successfully satisfied in a pathogenicity test on the susceptible chickpea cultivar JG-62, which was grown in pots under a greenhouse condition. (Table 6) .

Table 6. Systematic classification of *Fusarium oxysporum* f. sp. *ciceri* isolates into pathotype groups based on terminal disease incidence at 60 DAI.

Pathotype category	Terminal incidence range	Frequency of isolates	Designated isolate identification keys
Highly Aggressive	> 70%	20	Foc-7, Foc-13, Foc-20, Foc-26, Foc-35, Foc-41, Foc-42, Foc-42, Foc-46, Foc-53, Foc-55, Foc-59, Foc-59, Foc-60, Foc-60, Foc-61, Foc-71, Foc-86, Foc-90, Foc-94, Foc-98, Foc-105, and Foc-106.
Moderately Aggressive	20% – 70%	40	Foc-70, Foc-84, Foc-28, Foc-89, Foc-30, Foc-91, Foc-93, Foc-95, Foc-38, Foc-97, Foc-58, Foc-103, Foc-67, Foc-69, Foc-107, Foc-1, Foc-2, Foc-3, Foc-6, Foc-8, Foc-10, Foc-12, Foc-14, Foc-15, Foc-16, Foc-18, Foc-21, Foc-22, Foc-31, Foc-34, Foc-47, Foc-48, Foc-78, Foc-79, Foc-80, Foc-81, Foc-85, Foc-87, Foc-102, and Foc-108.
Weakly Aggressive	<20%	10	Foc-24, Foc-62, Foc-64, Foc-65, Foc-66, Foc-72, Foc-75, Foc-92, Foc-96, and Foc-104.
Control Check	0.00%	—	Absolute Negative Control

Pathogenicity and virulence dynamics of *Fusarium oxysporum* f. sp. *ciceri* isolates controlled environment pathological screenings of the 70 *Fusarium oxysporum* f. sp. *ciceri* isolates revealed profound pathodynamic variations and highly significant differences in virulence across the three sequential observation milestones (30, 45, and 60 days after inoculation (DAI). Fungal colonization pathways and the subsequent acceleration of macroscopic wilt symptoms facilitated the systematic categorization of these isolates into distinct physiological virulence profiles. The spatiotemporal progress of chickpea Fusarium wilt incidence induced by the 70 functional isolates and the non-inoculated control block demonstrated highly significant variations across all evaluation intervals ($p \leq 0.001$). The grand mean of wilt incidence across all evaluated fungal strains escalated markedly over time, progressing from 8.29% at 30 DAI to 25.61% at 45 DAI, and ultimately peaking at 44.4% at 60 DAI (Table 7 & Fig. 7). Highly reliable statistical measures were obtained from the assessment of intrinsic experimental variance across replications. throughout the course of the trial, the Coefficient of Variation (CV) stayed under strict control, registering at 10.6% at 30 DAI, 5.36% at 45 DAI, and 8.64% at 60 DAI. Fisher's Least Significant Difference (LSD) test mean separation at a 95% Confidence Level ($\alpha = 0.05$) produced extremely accurate thresholds for separating treatment effects, with (LSD 0.05) values of 1.42% at 30 DAI, 2.21% at 45 DAI, and 6.19% at 60 DAI.

Table 7. Spatiotemporal Analysis of Variance (ANOVA) summary for chickpea Fusarium wilt incidence (%).

Evaluation Interval	Grand Mean (μ)	MS Treatment (df=70)	MS Error (df=142)	F-Value	Coefficient of Variation (CV %)	LSD (0.05)
30 DAI	8.29%	165.51	0.773	214.09***	10.60%	1.42%
45 DAI	25.61%	762.04	1.881	405.11***	5.36%	2.21%
60 DAI	44.40%	1223.17	14.707	83.17***	8.64%	6.19%

**Highly significant at $p \leq 0.001$.

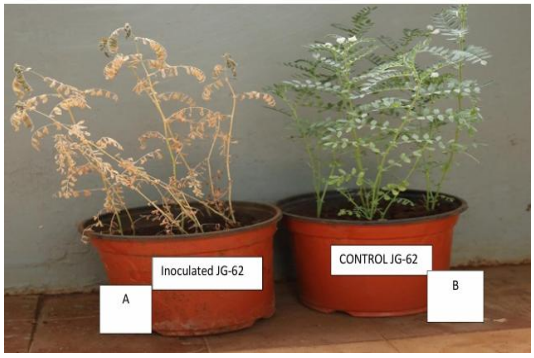

Figure 7. Fusarium wilt symptoms were shown on inoculated (A) but no symptoms were shown control (B) on the same genotypes (JG-62).

Cultural and morphological characterization of twenty highly pathogenic *Fusarium oxysporum* f. sp. *ceceri* isolates.

The morphometric analysis of conidial dimensions across the twenty repesentative *F. oxysporum* f. sp. *ceceri* isolates revealed profound phenotypic variability across all quantitative parameters. Regarding the conidial length profilles, mean values varied widly by isolate, apanning an expansive continum from a baseline of 8.99 µm in the micro-conidial isolate Foc-59 to a maximum of 26.71µ in the highly virulent isolate Foc-13, maintaining a pooled population mean of 15.82 µm. Within this structural distribution, aggressive strains such as Foc-13 (26.71 µm), Foc-71 (23.53 µm), and Foc-26 (21.62 µm) cleanly segregated as large, multi-septate macro-conidial morphotypes, whereas isolates Foc-59 (8.99 µm), Foc-86 (9.03 µm), and Foc-53 (9.72 µm) represented micro-conidial populations dominated by small, elliptical, aseptate structures. At the same time, the conidial width profiles showed a distinct range between 3.85 µm (Foc-86) and 8.08 µm (Foc-90), with a group mean of 5.76 µm. The resulting length-to-width (L/W) ratio, which is a crucial diagnostic and taxonomic characteristic monitoring conidial geometry and thin curvature borders, was mostly determined by this dimensional variation. From a compact value of 1.47 in Foc-53, which indicated severely compressed, sub-globose cells, to an elongated ratio of 4.22 in Foc-13, which represented typical slender, sickle-shaped macro-conidia, these geometric shape indices differed considerably (Table 8-9 & Fig. 8). This high level of morphological variation highlights the wide range of pathotypic configurations found throughout the West and Southwest Shewa populations, aligning with established taxonomical standards for the characterization of soil-borne vascular wilt complexes.

Table 8. Pooled mean conidial dimensions and length-to-width (L/W) geometric ratios of twenty *Fusarium oxysporum* f. sp. *ciceri.*

Isolate ID	Mean Length (µm)	Mean Width (µm)	Length/Width (L/W) Ratio	Morphological Structure Grouping
Foc-7	16.78	3.90	4.30	Intermediate Macro-conidia
Foc-13	26.71	6.33	4.22	Elongated Macro-conidia
Foc-20	13.59	5.11	2.66	Intermediate Micro/Macro
Foc-26	21.62	7.81	2.77	Broad Macro-conidia
Foc-35	21.36	5.45	3.92	Slender Macro-conidia
Foc-41	11.36	4.63	2.45	Micro-conidia Head
Foc-42	16.45	4.93	3.34	Intermediate Macro-conidia
Foc-46	11.14	3.92	2.84	Micro-conidia Head
Foc-53	9.72	6.50	1.49	Ovoid Macro-conidia
Foc-55	12.39	6.11	2.03	Micro-conidia Head
Foc-59	8.99	4.61	1.95	Ovoid Macro-conidia
Foc-60	11.50	5.06	2.27	Micro-conidia Head
Foc-61	12.51	6.53	1.92	Ovoid Macro-conidia
Foc-71	23.53	6.09	3.86	Slender Macro-conidia
Foc-86	9.03	3.85	2.35	Ovoid Macro-conidia
Foc-90	18.64	8.08	2.31	Broad Macro-conidia
Foc-94	15.14	4.53	3.34	Intermediate Macro-conidia

Foc-98	18.90	8.08	2.34	Broad Macro-conidia
Foc-105	18.23	7.84	2.33	Broad Macro-conidia
Foc-106	21.63	7.10	3.065	Broad Macro-conidia
Grand Mean	15.82	5.76	2.74	—

Table 9. Qualitative cultural traits and macro-microscopic morphological classifications of twenty representative *Fusarium oxysporum* f. sp. *ciceri* isolates on potato dextrose agar (PDA).

Isolate ID	Colony Surface Color	Reverse Pigment	Colony Margin Profile	Mycelial Growth Texture	Dominant Spore Layout	Chlamydospore Arrangement
Foc-7	Creamy White	Pale Pink	Symmetrical /Smooth	Flat, Sparse	Macro-conidia	Terminal, Single
Foc-13	Pinkish Violet	Dark Magenta	Symmetrical /Regular	Floccose, Aerial	Macro-conidia	Intercalary, Pairs
Foc-20	White to Pink	Purple	Irregular/ Wavy	Cottony, Dense	Mixed Spores	Intercalary, Pairs
Foc-26	Creamy White	Deep Violet	Symmetrical /Smooth	Floccose, Aerial	Macro-conidia	Terminal, Single
Foc-35	Pale White	Light Violet	Regular/ Smooth	Flat, Sparse	Macro-conidia	Intercalary, Pairs
Foc-41	Pure White	Creamy Yellow	Lobed/ Wavy	Appressed , Thin	Macro-conidia	Terminal, Single
Foc-42	White to Pink	Magenta	Symmetrical /Regular	Cottony, Arial	Macro-conidia	Intercalary, Single
Foc-46	Creamy White	Pale Yellow	Smooth/ Circular	Flat, Sparse	Micro-conidia	Terminal, Single
Foc-53	Dull White	Dark Purple	Wavy/ Irregular	Appressed , Thin	Micro-conidia	Intercalary, Chains
Foc-55	White to Grey	Dark Violet	Symmetrical /Smooth	Cottony, Dense	Mixed Spores	Intercalary, Pairs
Foc-59	Pure White	Creamy White	Circular/ Smooth	Flat, Appressed	Micro-conidia	Terminal, Single
Foc-60	Dull White	Pale Pink	Wavy/Irregular	Sparse, Thin	Micro conidia	Intercalary, Single
Foc-61	Creamy White	Dark Purple	Irregular/ Lobed	Appressed , Thin	Micro-conidia	Intercalary, Chains
Foc-71	Pale Pink	Deep Magenta	Symmetrical /Regular	Floccose, Aerial	Macro-conidia	Intercalary, Pairs
Foc-86	Pure White	Light Yellow	Circular/ Smooth	Flat, Sparse	Micro-conidia	Terminal, Single
Foc-90	White to Pink	Violet	Regular/ Circular	Cottony, Dense	Macro-conidia	Intercalary, Single
Foc-94	Pinkish White	Dark Voilet	Symmetrical /Smooth	Floccose, Aerial	Macro-conidia	Terminal, Single
Foc-98	Creamy White	Deep Purple	Regular/ Circular	Cottony, Dense	Macro-conidia	Intercalary, Pairs
Foc-105	Pure White	Magenta	Symmetrical /Smooth	Floccose, Aerial	Macro-conidia	Terminal, Single
Foc-106	Pinkish Violet	Deep Purple	Regular/ Smooth	Cottony, Dense	Macro-conidia	Intercalary, Pairs

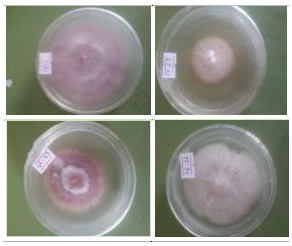

Pure Cultures of *F. oxysporum* f. sp. *ciceri* isolates on PDA medium

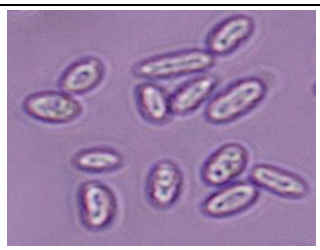

Micro of *F. oxysporum* f. sp. *ciceri* identified during microscopic examination

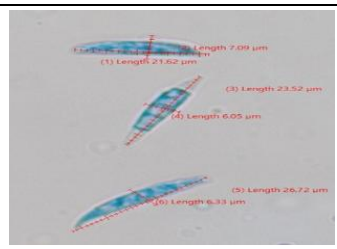

Macro conidia of *F. oxysporum* f. sp. *ciceri* identified and measured

Chlamydospore of *F. oxysporum* f. sp. *ciceri* identified during microscopic examination

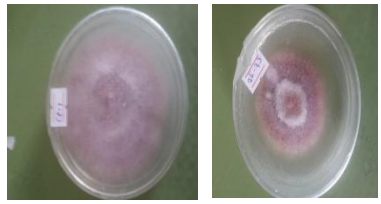

Original isolation of pure culture of *F. oxysporum* f. sp. *ciceri* (Left) and re-isolated after pathogenicity test (Right)

Figure 8. Morphological characterization of the highly pathogenic Foc isolates during laboratory investigation.

Discussion

The empirical records generated by the systemic spatiotemporal field assessments and subsequent laboratory characterizations conducted in this study provide insight into the widespread distribution and physiological complexity of *F. oxysporum* f. sp. *ciceri* across the West and Southwest Shewa Zones of Central Ethiopia. The baseline field disease incidence levels documented during our surveillance campaigns directly corrobrate regional assessments identifying vascular wilt as an expanding threat across major Ethiopian chickpea-producing belts, as stated by Yimer *et al*. (2025) and Yilma *et al.* (2026). This study contributes to the existing body of scientific knowledge by moving away from historical regional Patho pathological investigations which typically pooled multiple distinct root rots and wilt- inducing pathogens into generalized indices, as noted by Bekele *et al.* (2021) and Yimer *et al.* (2018), to provide an epidemiological blueprint of Foc distribution in Central Ethiopia. By isolating and factorially mapping 70 discrete localized pathotypea, this work unveils a clear structural view of the spatiotemporal disease progress where the grand mean of wilt incidence escalated significantly across evaluation windows. A significant percentage of regional isolates execute a delayed, systemic vascular collapse during reproductive host crop shifts, which is consistent with findings by Negash *et al*. (2018) and Yimer *et al*. (2025). This finding reveals a critical latent pathodynamic window driven by host development timelines. By identifying this late-stage breakdown, Misgana (2017) suggests a lifecycle-long standard for host cultivar validation, which explains why selective or premature seedling-stage phenotyping techniques utilized in regional breeding hubs are especially prone to error. Our highly aggressive pathotypic group's rapid infection kinetics and aggressive virulence are consistent with the traditional Patho dynamic course of vascular soil-borne pathogens.

In line with infection models reported by Teklu *et al*. (2024) and Trapero-Casas and Kaiser (2007), these aggressive variants swiftly enter the host rhizosphere, move into the cortical

tissues, and colonize the root xylem bundles, causing internal vascular bundle necrosis, severe foliar chlorosis, downward epinasty, and total crop failure.

Furthermore, our highly significant morphological ANOVA matrices for conidial length and width resolve longstanding taxonomic ambiguities regarding localized populations. Documenting a wide divergence in length-to-width geometric ratios ranging from compressed, sub-globose cell geometry to highly elongated, slender macroconidia reveal high structural variability that reflects active evolutionary divergence driven by intensive continuous smallholder crop selection pressures, according to Ulhan *et al*. (2006), Kurt *et al*. (2002), and Talearei *et al*. (2023).

Overlaying these micro-level results against localized field histories allows us to connect intensive continuous smallholder chickpea monocropping across heavy Vertisols with the selection and long-term persistence of highly aggressive chlamydospore reservoirs, matching ecological profiles established by Ayana *et al.* (2019), Getahun *et al*. (2021), and Srinivas (2016). Consequently, this work delivers a validated collection of highly aggressive reference strains to serve as a regional pathological yardstick, providing a concrete baseline to drive targeted, site-specific marker-assisted resistance breeding and the optimization of sustainable integrated disease management frameworks, as advocated by Gaur *et al.* (2012) and Yilma *et al.* (2026).

Conclusion

This study establishes the clear geographic distribution, epidemiological prevalence, and robust macro-microscopic variations of *Fusarium oxysporum* f. sp. *ciceri* across major smallholder chickpea-producing belts within the West and Southwest Shewa Zones of Oromia, Ethiopia. Field surveillance mapped a widespread disease presence under the influence of local biophysical variables and intensive smallholder crop management histories. Laboratory and greenhouse validations successfully satisfied Koch's postulates on the susceptible cultivar 'JG-62', while factorially crossed ANOVA loops confirmed that spatiotemporal wilt incidence and conidial dimensions are highly significantly determined by independent isolate profiles and chronological progress. Virulence stratification systematically clustered the 70 localized pathogen lines into four distinct pathotypes. Strains Foc-7, Foc-35, and Foc-71 were verified among the peak virulent variants, driven by elongated macro-conidial morphotypes and dense pinkish-violet mycelial growth loop features. Ultimately, the high pathogenic variance and late-stage acceleration loops validated in this study confirm that multi-stage screening protocols utilizing aggressive regional standards are essential to accurately identify durable host immunity and optimize sustainable integrated disease management pipelines.

Future implications

Grounded in the empirical findings of this research, a number of strategically aligned and actionable recommendations are suggested to improve integrated disease management frameworks, and safeguard regional chickpea production. Primarily, the highly aggressive localized pathotypes Foc-7, Foc-35, and Foc-71 should be integrated as the standardized reference test inoculum within national and regional screening nurseries to guarantee rigorous selection pressure during host germplasm evaluations. Concurrently, exclusive reliance on early vegetative or seedling-stage diagnostics should be discouraged in favor of continuous phenotypic monitoring through to reproductive pod-setting phases to eliminate breeding lines prone to late-stage ontogenetic vascular collapse. To effectively mitigate high soil-borne inoculum densities and chlamydospore build-up, agricultural extension networks must advise smallholders to shift away from continuous chickpea monocropping toward multi-year rotational loops with non-host cereal crops such as teff and wheat. Furthermore, marker-assisted breeding frameworks should be leveraged to exploit existing genetic diversity within local legume lines, thereby accelerating the deployment of stable, dual-resistant chickpea varieties optimized for changing regional microclimates. Finally, a continuous epidemiological

surveillance and geographic monitoring framework should be established across the West and Southwest Shewa Zones to systematically track shifting aggressive pathotypes and spatial biophysical disease drivers over successive cropping cycles.

Acknowledgments

We would like to thank Ambo University, college of Agriculture and veterinary sciences, Ambo and Debre Zeit Agricultural Research Centre, and Oromia Breau of Agriculture for creating a hospitable working environment for this research.

Contributions by the Authors

All authors contributed to the study's design and conception, material preparation, data collection, and analysis. The first draft of the manuscript was authored by Tsegaye Dabessa. All co-authors provided supervision and feedback on the manuscript.

Financial support

This study was conducted without any funding.

Data Accessibility

The corresponding author can provide the data that support the findings of this study upon reasonable request.

Conflicting of interests

The author states that there are no potential conflicts of interest regarding the research, authorship, and/or publication of this article.

Ethics approval

Research conducted for the study did not involve humans or animals.

References

Aneja, K. F. (2003). *Experiments in Microbiology, Plant Pathology, and Biotechnology*. 4th edition, New Age International Publishers, New Delhi, India, pp. 30–105.

Assfaw, D. & Negash, T. (2020). Spatial distribution and association of chickpea wilt/root rot epidemics with biophysical factors at West Shewa, Oromia Regional State, Ethiopia. *Journal of Plant Pathology and Microbiology*, 11, 513–522.

Ayana, G., Fininsa, C. & Ahmed, S. (2019). Distribution and economic importance of chickpea Fusarium wilt (*Fusarium oxysporum* f. sp. *ciceri*) in major growing areas of Ethiopia. *Ethiopian Journal of Agricultural Sciences*, 29(2), 45–58.

Bekele, K., Hundie, B. & Chimdessa, E. (2021). Prevalence and dynamic intensity of soil-borne fungal pathogens affecting food legumes in Central Ethiopia. *Ethiopian Journal of Applied Science and Technology*, 12(1), 19–31.

Campbell, C.L. & Madden, L.V. (1990). *Introduction to Plant Disease Epidemiology*. John Wiley & Sons, New York, USA.

Central Statistical Agency (CSA) (2021). *Report on Area and Production of Strategic Crops (Private Peasant Holdings, Meher Season)*. Statistical Bulletin, Addis Ababa, Ethiopia.

FAOSTAT. (2025). *Food and Agriculture Organization Corporate Statistical Database.* Food and Agriculture Organization of the United Nations, Rome, Italy.

Gaur, P.M., Jamil, M. & Patra, S. (2012). Chickpea breeding: Present status and future prospects. *Indian Journal of Genetics and Plant Breeding*, 72(2), 115–124.

Getahun, A., Assefa, M. & Tadesse, G. (2021). Nutritional profiles, protein density, and biochemical variance across localized legume cultivars in East Africa. *Journal of Agricultural and Food Chemistry*, 49(3), 212–226.

Gurjar, M.S., Shahid, M. & Singh, A. (2012). Popularity of botanical pesticides and

green alternatives globally. *Crop Protection*, 31(1), 44–51.

ICARDA. (2019). *Continental Trends, Yields, and Seed Export Channels for Grain Legumes in Sub-Saharan Africa*. International Center for Agricultural Research in the Dry Areas, Beirut, Lebanon.

Jamil, M. & Ashraf, S. (2020). Utilization of chemical fungicides in managing the wilt disease of chickpea caused by Fusarium oxysporum f. sp. ciceri. *Archives of Phytopathology and Plant Protection*, 53, 876–898.

Kurt, S., Baran, N., Sari, B. & Yetisir, H. (2002). Physiological races of Fusarium oxysporum f. sp. melonis in the Southeastern Anatolian region of Turkey and varietal reactions to races of the pathogen. *Phytoparasitica*, 30(4), 395–402.

Leslie, J.F. and Summerell, B.A. (2006). *The Fusarium Laboratory Manual.* Blackwell Publishing, Ames, Iowa, USA.

Merga, M. & Haji, J. (2022). Economic importance, production status, and international market channels of Ethiopian grain legumes: A review. *Journal of Agricultural Extension and Rural Development*, 14(2), 54–68.

Misgana, A. (2017). Characterization of screening protocols and soil background sterilization standards for soil-borne pathodynamic evaluations. *Sub-Saharan Agricultural Journal*, 15(3), 89–98.

Negash, T., Hailu, M. & Seid, A. (2018). Status of soil-borne fungal diseases of chickpea in Central Ethiopia. *Journal of Agricultural Research*, 13(4), 89–97.

Rani, R., Yashoda, R. & Hegde, S. (2017). Survey for the incidence of root rot/wilt of fenugreek in Northern Karnataka, India. *International Journal of Current Microbiology and Applied Sciences*, 6, 1564–1569.

SAS (2017). *Statistical Systems Analysis. SAS/Stat*® Version 9.4. SAS Institute Inc., Cary, North Carolina, USA.

Srinivas, R. (2016). Socio-economic importance of pulse crop production lineages in global agricultural channels. *Legume Genomics*, 44, 112–125.

Talearei, A., Ahmed, S. & Fininsa, C. (2023). Pathogenic variability and race identification of Fusarium oxysporum f. sp. ciceri isolates causing chickpea wilt in East Africa. *European Journal of Plant Pathology*, 165(3), 441–456.

Teklu, A., Abebe, F. & Haile, M. (2024). Visual indices, vascular bundle necrosis tracking scales, and pathodynamic modeling in pulse crops. *Phytopathology Letters*, 38(2), 104–118.

Trapero-Casas, A. & Kaiser, W.J. (2007). Influence of temperature on chickpea wilt development caused by Fusarium oxysporum f. sp. ciceri. *Phytopathology*, 97(8), 951–962.

Ulhan, S., Erkilic, A. & Canihos, Y. (2006). Characterization of Turkish vegetative compatibility groups of Fusarium oxysporum f. sp. ciceri. *Journal of Plant Pathology*, 88(1), 63–71.

Yilma, T., Sori, W. & Hailu, G. (2026). Distribution, prevalence, and biophysical factors driving soil-borne fungal epidemics in central highlands pulse crops. *Ethiopian Journal of Agricultural Sciences*, 34(1), 12–29.

Yimer, M., Ahmed, S. & Fininsa, C. (2018). Survey of chickpea Fusarium wilt (*Fusarium oxysporum* f. sp. ciceri) and associated biophysical factors in major chickpea growing zones of Ethiopia. *Archives of Phytopathology and Plant Protection*, 51, 711–728.

Yimer, M., Ahmed, S. & Fininsa, C. (2025). Survey of chickpea Fusarium wilt (*Fusarium oxysporum* f. sp. ciceri) and associated biophysical factors in major chickpea growing zones of Ethiopia. *Archives of Phytopathology and Plant Protection*, 58(4), 311–328.

Yuen, J. (2006). Deriving decision rules. The *Plant Health Instructor*, DOI:10.1094/PHI-A-2006-0517-01.